

Experimental behaviour of high-performance concrete in confined tension

Fabrice Dupray  Yann Malecot 
Laurent Daudeville

Received: 1 October 2008 / Accepted: 13 July 2009 / Published online: 25 July 2009
© RILEM 2009

Abstract Prestressed concrete is commonly used in a wide range of applications, yet on rare occasions

spalling problems have been reported for concrete structures prestressed in two directions. The behaviour of concrete may be affected by prestress-main features of this technology consist of limiting ing; consequently a number of experiments have been both the tensile areas in bent concrete sections and the performed to reproduce this load combination on macroporosity of a concrete structure by closing the laboratory samples. Tests were carried out in a tensile cracks located in it. Even though it is widely compression-tension triaxial cell suitable for the used, some applications may reveal rather unusual independent application of a lateral confining pres- problems. In the case of a two-direction prestress, sure, as well as a direct axial tension load. Results spalling has only rarely been reported, which means reveal a measurable but limited reduction in concrete that in the external area of the structure (between the tensile strength with a confining pressure of a similar prestressing cables and external surface), concrete magnitude as the prestress (order of magnitude of blocks become detached from the structure. Even 10 MPa). Further experiments were conducted at though this phenomenon does not affect short-term higher confining pressures, in both confined tension structural stability, corrosion problems may arise in and in triaxial extension, in order to generate an the long term and air or water tightness of the structure overview of limit state behaviour for the studied high may be adversely affected: the spalling phenomenon performance concrete. therefore must be prevented.

Keywords High-performance concrete
Tensile properties Experimental tests
Confined tension Triaxial extension
Limit states

This study is aimed at characterising the concrete behaviour in confined tension (CT), as well as identifying the effect of prestress on tensile strength and evaluating the ability of typical criteria to predict this limit state. Since such loadings primarily concern prestressed concrete, a high-performance concrete (HPC), has been chosen for study given its wide-spread use in most prestressed structures.

Experimental biaxial tests have been conducted on concrete plates by Hussein [1] and others, while hydraulic fracturing in confined tension has been studied by Visser [2]. Moreover, the behaviour in

F. Dupray · Y. Malecot (✉) · L. Daudeville
Université Joseph Fourier - Grenoble 1, Laboratoire 3S-R,
BP 53, 38041 Grenoble Cedex 9, France
e-mail: yann.malecot@ujf-grenoble.fr

F. Dupray
e-mail: fabrice.dupray@univ-savoie.fr

triaxial extension of various medium-strength concretes under similar confinement (between $17 \times 10 \times 40$ cm beams. All results shown are for an 69 MPa) has been studied by Kotsovos and Pavlovic [3] and Newman [4]. To the best of our knowledge however, no experiment has ever been conducted on the tensile behaviour of a high-performance concrete under a wide range of lateral confining pressures (i.e. from 10 to 250 MPa).

The series of tests performed will be described and their results presented in the next three sections: uniaxial tests in Sect. 2, confined tensile tests in Sect. 3 and extension tests in Sect. 4. An analysis of results plus a comparison with some typical triaxial extension criteria will then be discussed in Sect. 5. As for notation, σ_1 is the axial stress, P_c the confining pressure, p the mean pressure, and σ_d the differential stress. For purposes of the present article, these values are all considered to be positive when in compression.

2 Uniaxial characterisation

2.1 Material and samples

The mixture of the studied concrete is given in Table 1. Both the uniaxial compression (UC) on small concrete cylinders, and the three-point-bending (TPB) tests on small concrete beams were performed in order to characterise the uniaxial behaviour of this particular concrete. The material characteristics, including compressive strength, Young's modulus, Poisson's ratio and tensile strength, have been identified from these test results.

All the CT and UC tests were carried out on 10×20 cm cylindrical samples that were cored, cut

Table 1 Composition of the studied HPC

| Element | Proportion (kg/m ³) |
|--------------------|---------------------------------|
| Limestone sand 0/5 | 780 |
| Fine gravel 5/12.5 | 320 |
| Gravel 12.5/25 | 810 |
| Limestone fillers | 60 |
| Silica fumes | 40 |
| Water | 160 |
| CEM II 42.5 cement | 265 |
| Superplasticiser | 9 |

2.2.1 UC tests

For these tests, the samples were instrumented with three strain gauges (two of them are axial and the other is circumferential). A ball joint and accurate alignment were used to avoid bending. The displacement of the press plates was measured with three LVDT sensors. Three tests were performed to characterise the compression strength of the HPC, with the mean compressive strength equalling 71.7 MPa. The mean peak deformation was 0.26%. The results of these tests are shown on Fig. 1. The stress-strain curves display an elastic-brittle behaviour which is typical for this kind of HPC.

2.2.2 Three-point-bending tests

Identifying the tensile behaviour of concrete by means of bending tests is a common practice; it allows recording the post-peak tensile behaviour with a stable displacement-controlled test, in addition to estimating the fracture energy. Instrumentation on the three tests

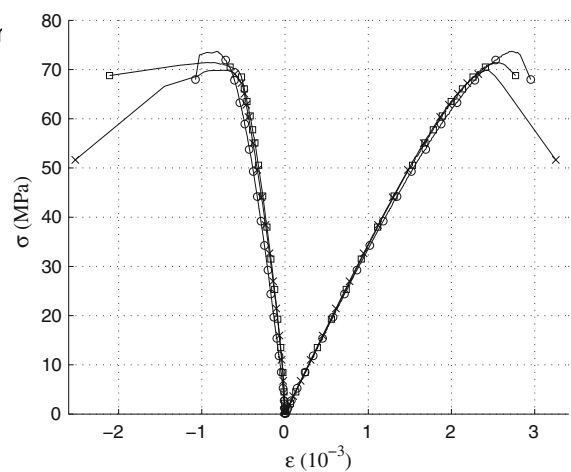


Fig. 1 Results of uniaxial compression tests: axial stress, σ_1 (axial, on the right) and σ_θ (circumferential, left)

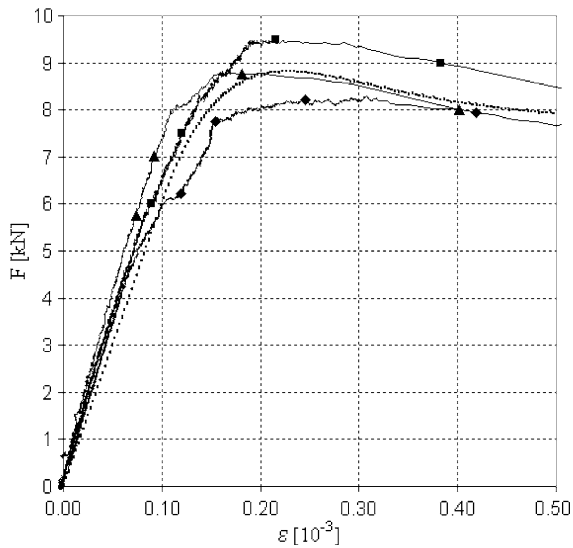


Fig. 2 Results of the TPB tests: bending load F vs. maximal longitudinal strain ε (solid lines) and the identified Mazars model (dotted line)

undertaken consisted of a strain gauge on the bottom side, where fracture should initiate, plus a set of five LVDT sensors for measuring displacements both at mid-span and on the other two loading points. Results are displayed on Fig. 2. Due to both the nonlinear constitutive behaviour of concrete and the inhomogeneous stress state in bending, tensile strength can be identified through simulation of the TPB test with a robust damage constitutive model for concrete, i.e. the Mazars model [4].

3 Compressed tensile tests

3.1 Experimental set-up

3.1.1 Triaxial cell

The same servo-hydraulic press has been used for all the compressed or unconfined tests. The Schenck Hydropuls press has a capacity of 1,000 kN and contains a very accurate force sensor. The compression unit is able to generate a compressing pressure of up to 70 MPa via a pressure multiplier. The compression fluid is a hydraulic oil for high pressure systems. The cell itself was modified from a conventional triaxial cell in order to be able to apply tensile stress on the sample.

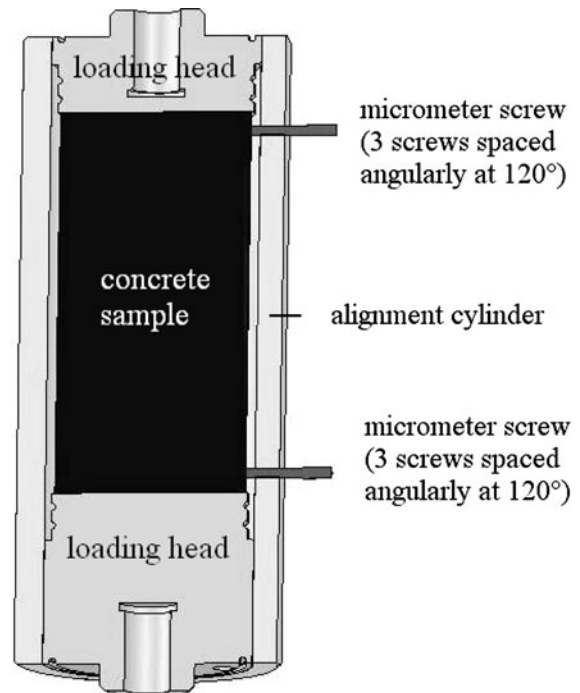


Fig. 3 Section cut of the alignment system

3.1.2 Bonding system

The adhesive Sikadur 30 is used to bond the concrete sample with the steel loading heads. A system was designed to bond the concrete specimen and loading heads in addition to offer alignment control (Fig. 3). This system consists of a hollow cylinder fitted with six micrometre screws to ensure alignment and parallelism. The limitation therefore is only set by the geometrical flaws of the sample, which remain relatively small. Over the bonding zone, an adhesive crown allows reducing stress concentration effects (see Fig. 4). No rupture was observed within this zone when using the given system.

3.1.3 Strain measurements

Strain measurements have been conducted by means of two axial gauges and one circumferential gauge. An LVDT sensor was placed outside the cell between the press plates so as to ensure that gauge measurements were correct. Since maximum aggregate size equals roughly 2 cm, 5-cm gauges were used to guarantee a homogeneous strain measurement.

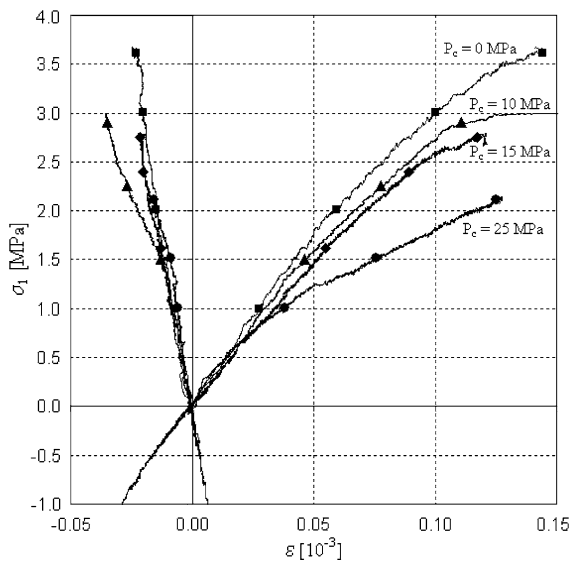


Fig. 7 Confined tensile tests—tensile behaviour comparison at various confining pressures: axial stress vs. axial (right side) and circumferential (left) strains ϵ

therefore maintains a tensile strength similar to that of ordinary concretes, and above 2 MPa, and the spalling observed cannot simply be explained by the biaxial compression stress state.

4 Extension test

4.1 Experimental protocol

In order to obtain a more comprehensive view of the behaviour of this HPC study specimen under triaxial load paths with one direction in extension, an additional test was conducted. The press used for this test, called the Giga press, offers a much higher capacity than the Schenck press: it is able to apply a mean pressure above 1 GPa on concrete cylinders with a 7-cm diameter and 15.5 cm high. The Giga press, specifically designed for triaxial compression tests, can also perform extension tests but not tensile tests. A much higher confining pressure is applied during the extension test in order to broaden the study range, and this pressure also serves to avoid entering

into the tensile area at the end of the load path, which is beyond the limitations of the press. Pressure was set equal to 250 MPa, and the load path is shown in Fig. 8.

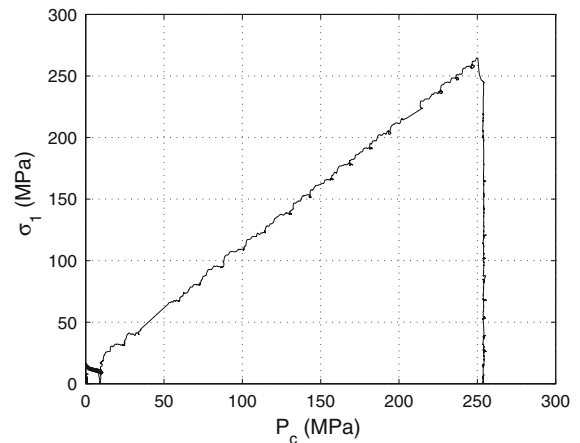


Fig. 8 Triaxial extension test load path: axial stress vs. confining pressure P_c

4.1.1 Strain measurements

As opposed to what is often stated, such as in Schmidt [8], it remains possible to obtain reliable measurements from gauges at very high pressure provided the appropriate protection system is used, as demonstrated by Gabet [6] and Vu [9]. Strain measurements proceed by means of an axial LVDT sensor, combined with one axial gauge and two circumferential gauges. This set-up therefore differs slightly from that used on the confined tensile tests. The gauges are only slightly longer than the maximal aggregate size of the concrete. The two circumferential gauges prove necessary due to the inhomogeneity of the concrete sample. The mean value of the two circumferential gauges will thus be considered for all subsequent graphs.

4.1.2 Sample protection

The impacts of a higher confining pressure must be prevented by introducing stronger protection. The principle remains the same as in confined tension (see Sect. 3.1.4), but the multilayer protective latex membrane is now 6 mm thick, with an additional 1 mm of neoprene.

4.2 Tests results

Figure 8 shows the load path for this extension test; This path differs from that used for the confined tensile tests. It begins by a quasi-hydrostatic loading,

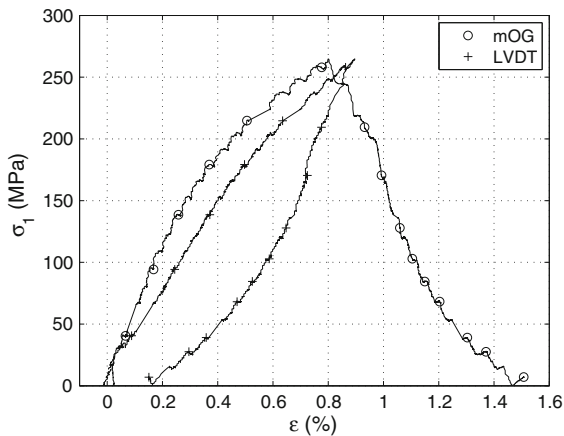


Fig. 9 Triaxial extension test: axial stress vs. axial (LVDT) and circumferential (mean circumferential gauge mOG) strains ϵ

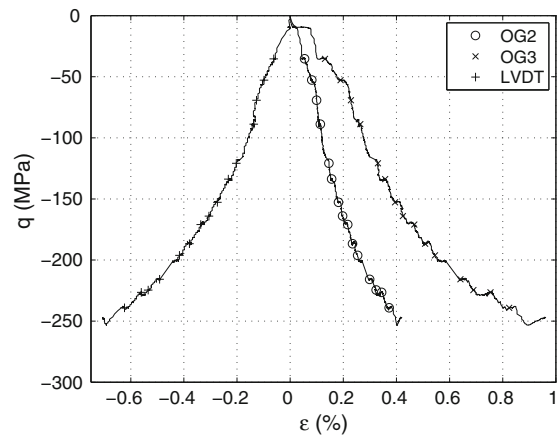


Fig. 11 Triaxial extension test: deviatoric phase: deviatoric stress q vs. axial (LVDT) and circumferential (OG2 and OG3) strains ϵ , from which the hydrostatic strain can be deduced

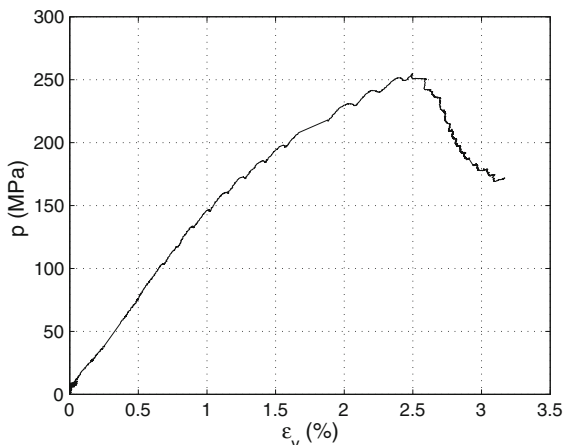


Fig. 10 Triaxial extension test: mean stress p vs. volumetric strain ϵ_v

which show that this linear phase lasts about up to a stress roughly twice the simple compressive strength. Volumetric behaviour ($\epsilon_v = \epsilon_1 + \epsilon_2 + \epsilon_3$) is contracting from the beginning of triaxial unloading (see Fig. 10), and heavily contracting by the end of the test. The opposing effects of a decrease in mean stress $p = \sigma_m = 1/3 \times (\sigma_1 + 2P_c)$ (dilating effect) and an increase in absolute value of differential stress $q = \sigma_1 - P_c$ (contracting effect) lead to a contracting effect, even if only the circumferential gauge with minimal strains (OG2, see Fig.1) is taken into account when calculating volumetric behaviour ($\epsilon_v = \epsilon_1 + 2 \times \epsilon_2$).

with lateral pressure being directly set by a fluid, while the equivalent axial pressure is reproduced using the axial jack. Stress on the axial jack then drops slowly. The loading rate during the hydrostatic phase equals 0.45 MPa/s, and during the extension phase, the strain rate is $7.10s^{-1}$.

Figure 9 provides results of the extension test in terms of axial stress vs. axial and circumferential strains. Figure 10 exhibits the volumetric behaviour of this sample for the same test. This figure displays a rather long linear phase during the hydrostatic part of the loading, up to 150 MPa of confinement. This value can be compared with the results obtained by Gabet [10] and Schmidt [8] in their respective works,

5 Analysis of the test results

5.1 Effect of the confinement on the tensile behaviour

The effect of confinement on tensile strength can be analysed within a stress space. Figure 12 shows the tensile strength under both confined and unconfined tests into the (p, q) plane, where p is the mean stress $\frac{\sigma_1 + 2P_c}{3}$ and q is the differential stress $\sigma_1 - P_c$. It is worthwhile to note that all four points are well aligned. Moreover, the uniaxial compression test underscores that the yield surface in triaxial compression is significantly higher than in extension (Fig. 2). This result confirms that the tensile or extension meridian of the yield surface for concrete is lower (closer to the



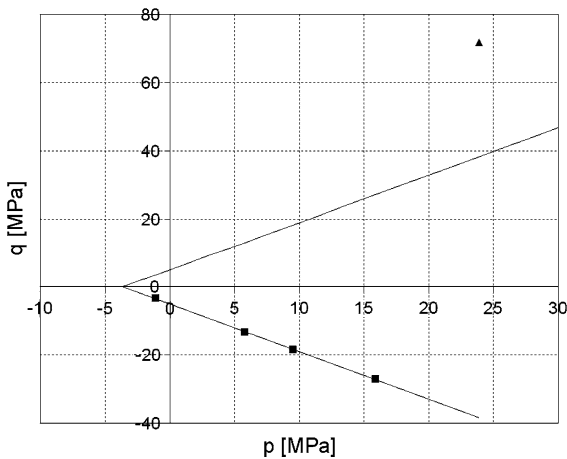


Fig. 12 Limit-states in the p - q plane (square), as observed under confined tension. Linear approximation and its symmetric part in triaxial compressions (solid lines), compared with uniaxial compression (triangle)

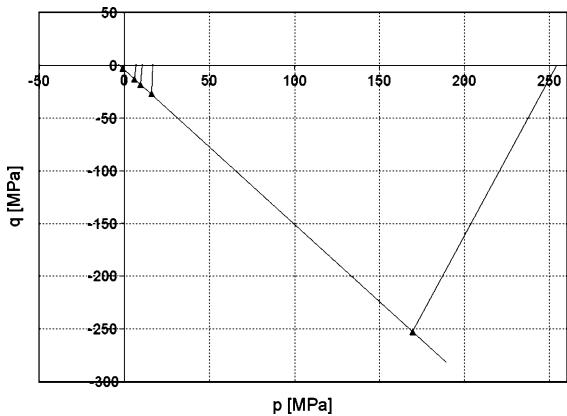


Fig. 13 Representation of limit-states in the p - q plane of confined tension and extension tests (triangle), with the corresponding linear approximation (solid line)

hydrostatic axis at the same pressure) than the compressive meridian, as explained by Chen [1], and observed by Kotsovos [3] and by Jiang et al. [2], albeit with a very different setup.

5.1.1 Comparison between confined tension and extension

The remarkable alignment of the limit-states in confined tension has been confirmed at higher mean stresses. Although its load path differs slightly, the extension test performed at a confining pressure of 250 MPa clearly confirms the trend, as can be seen in

Fig. 13. Up until this stress level, the failure limit of this HPC can be approximated with a few of the more typical linear yield criteria, yet not with parabolic criteria.

5.1.2 Comparison with other confined tension and triaxial extension tests

The only results from comparable studies on various concretes available in the literature were obtained by Kotsovos and Newman [8] and Mills and Zimmerman [14], as cited in [5]. Kotsovos' study combined three different concretes, characterised by their compression strength (32, 47 and 62 MPa), and different levels of confining pressure between 17 and 69 MPa. Results from the range of tests have been combined in q/f_c vs. p/f_c plane with great consistency between tests, and have been modelled by a power law approximation of failure states within this plane. The exponent for the triaxial extension meridian that Kotsovos identified lies close to 1, i.e. 0.86.

Results from the present study will now be combined with those obtained by Kotsovos and by Mills and Zimmerman in Fig. 14. Both of these studies are complementary in this depiction, since the confined tension tests performed on the HPC specimen exhibit a lower p/f_c ratio than the Kotsovos ratios, and since the extension test on HPC yields a much higher reference point. It then clearly appears that a linear approximation provides a good representation of the failure surface of all tested concretes within this q/f_c vs. p/f_c plane. Recent tests conducted

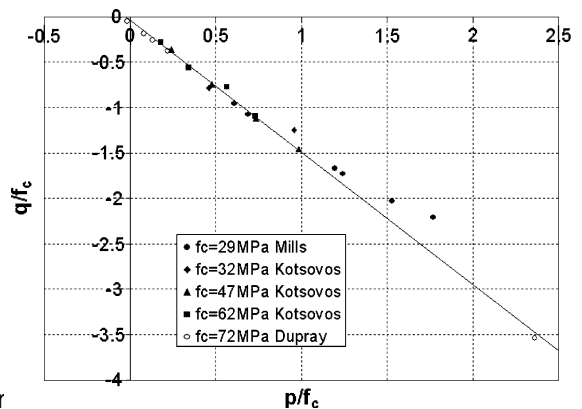


Fig. 14 Representation of the limit-states in the q/f_c vs. p/f_c plane for five concretes, along with their corresponding overall linear approximation



by Wang and Song [6] show that mass concretes with a high aggregate ratio have an extension meridian close to that shown here. These results have been obtained in confined tension and serve to confirm that this meridian is linear at low mean pressures.

Given that triaxial extension tests at high pressure are rare, it is impossible to extrapolate these results for normal strength concretes above $\sigma_1/\sigma_3 = 1$. A comparison however is possible with results from various experimental set-ups presented by Seow [17]. Such comparisons reveal that at higher levels of σ_1/σ_3 , the linear approximation is no longer valid. Though not interpreted in this manner by Seow, the compilation of results also clearly indicates that up to $P_c/f_c = 1$, the linear approximation remains valid. As seen in Fig. 13 however, this linear failure surface is also easily validated for the HPC specimen, at least up to a confining pressure of 250 MPa, which corresponds to $P_c/f_c = 3.6$. The potential difference between the various concretes lies in their respective volumetric behaviour. While normal strength concretes are usually dilating from the beginning of the deviatoric phase (see Kotsovos' tests [3]), in our HPC is obviously slightly contracting at high pressure level.

5.1.3 Comparison with typical models used in confined tension

It is well known that geomaterials are pressure dependant, which makes it straightforward therefore to analyse test results in the σ_1 - σ_3 plane where σ_1 is the mean stress and σ_3 is the von Mises stress. ($J = \sqrt{3}J_2$ where J_2 is the second deviatoric stress invariant). In the present study $J = |q|$ where $q = \sigma_1 - P_c$ is the differential stress. The analysis will be carried out in the q vs. p plane.

Plasticity models are often used to describe concrete behaviour, even for loadings that lead to the fragile rupture of concrete. Their respective advantages and drawbacks will not be discussed here, but it would still be interesting to check which models output a yield surface that is compatible with previous results. Model families are basically characterised by two criteria. First, the shape of the yield surface within a deviatoric plane can either be circular (no influence exerted by the Lode angle),

hexagonal (Tresca-derived criteria) or triangular with rounded angles (as introduced by Zienkiewicz et al. [18]). Second, the shape of the meridians can be linear (Drucker-Prager criterion [9] and its derivations) or curved (von Mises-Schleicher criteria and its derivations), without considering possible yield surface closure at very high pressures, which has not been investigated in this paper.

First of all, these tests have confirmed that the tensile meridian must be lower than the compressive meridian, which is a normally accepted finding (see Fig. 15), and can only be modelled through a yield surface that is roughly triangular in the deviatoric plane. These tests however also shed new light on the tensile behaviour of concrete under relatively low confinement (i.e. with $p/f_c < 1$). All tests performed and found in the literature tend to prove that the failure surface in strictly confined tension (i.e. $\sigma_1 < 0$ according to our signs convention) is linear.

For the tested HPC, the failure surface is linear up to a much higher pressure than that shown in results from Mills et al. [14] for an ordinary concrete ($f_c = 29$ MPa). Previous authors have demonstrated that the failure surface of an ordinary concrete tends to curve at moderate pressure confinement (≈ 1). Plasticity models using a parabolic criterion for low pressures are therefore not the best suited for modelling concrete failure in confined tension. This is especially true with the MSDP model, developed by Aubertin et al. [5], which is a blend of the von Mises-Schleicher criterion at low pressures with the Drucker-Prager criterion at higher pressures. Although this criterion seems to operate well in triaxial compression, previous results have shown that the opposite mix would be more accurate in triaxial extension. Recent upgrades of the Extended Leon Model (ELM) by Pivonka et al. [20] indicates the possibility of having a curvy yield surface that closely resembles a cone in the low pressure area. Such a criterion could offer a quite accurate solution for ordinary concretes, even those featuring relatively high-performance. But the simplest and most accurate model for describing the observed extension part of the failure surface is the three-parameter Willam-Warnke model [21]. The Drucker-Prager yield surface is simply modified to integrate a Lode angle dependency that reduces the failure level in either triaxial extension or confined tension, in comparison with the meridian for compressive triaxial stress states.



6 Conclusion

The tensile behaviour of a high-performance concrete under both very low confinement and under higher confinement has been investigated herein. Results appear to be in agreement with previous studies on normal concretes for the low confinement range, i.e. while the axial strength is tensile (<math>\sigma_1 < 0</math>). For such a confinement, the difference between ordinary concrete and high-performance concrete is not visible in the σ_1 - σ_2 vs. σ_1 - σ_3 plane. The typically curved tensile meridian of the limit state surface has not been encountered since the tensile meridian is linear up to a 250-MPa confinement. The observed spalling cannot be explained by a decrease in confined tension strength, which remains above 2 MPa in prestressed concrete.

When all stresses are compressive ($\sigma_1 > 0$), the HPC failure surface is still linear within the meridian plane. An investigation of the Lode angle influence, e.g. by means of triaxial compression testing, might help define a fully 3D failure and yield criterion for HPC. Such an approach could confirm whether the three-parameter Willam-Warnke criterion is accurate for only the tensile meridian or for both tensile and compressive meridians in the case of HPC.

References

- Hussein A, Marzouk H (2000) Behavior of high-strength concrete under biaxial stresses. *Mater J* 97:27–36
- Visser JHM, van Mier JGM (1998) The mechanical behaviour of hydraulic fractured, possibly saturated materials. In: Proceedings of fracture mechanics of concrete structures (FraMCoS-3). Gifu, Japan, pp 269–280
- Kotsovos MD, Pavlovic M (1995) Structural concrete: finite-element analysis for limit-state design. Thomas Telford, London
- Newman J (1974) Apparatus for testing concrete under multiaxial states of stress. *Mag Concr Res* 26:229–238
- Mazars J (1986) A description of micro- and macroscale damage of concrete structures. *Eng Fract Mech* 25(5):729–737
- Gabet T, Malecot Y, Daudeville L (2008) Triaxial behaviour of concrete under high stresses: influence of the loading path on compaction and limit states. *Cem Concr Res* 38(3):403–412
- Vu XH, Malecot Y, Daudeville L, Buzaud E (2009) Experimental analysis of concrete behavior under high confinement: effect of the saturation ratio. *Int J Solids Struct* 46:1105–1120
- Schmidt MJ, Cazacu O, Green ML (2008) Experimental and theoretical investigation of the high-pressure behavior of concrete. *Int J Numer Anal Methods Geomech* 33(1):1–23. doi:10.1002/nag.700
- Vu XH, Malecot Y, Daudeville L, Buzaud E (2009) Effect of the water/cement ratio on concrete behavior under extreme loading. *Int J Numer Anal Methods Geomech*. doi:10.1002/nag.796
- Gabet T, Vu XH, Malecot Y, Daudeville L (2006) A new experimental technique for the analysis of concrete under high triaxial loading. *J Phys IV* 134:635–640
- Chen WF (1982) Plasticity in reinforced concrete. McGraw-Hill, New York
- Jiang LH, Huang DH, Xie NH (1991) Behaviour of concrete under triaxial compressive-compressive-tensile stresses. *Mater J* 88(2):181–185
- Kotsovos MD, Newman JB (1979) A mathematical description of the deformational behaviour of concrete under complex loading. *Mag Concr Res* 31:77–90
- Mills L, Zimmerman R (1970) Compressive strength of plain concrete under multiaxial loading conditions. *ACI J* 67:802–807
- Aubertin M, Simon R (1998) Un critère de rupture multiaxial pour matériaux fragiles. *Can J Civ Eng* 25:277–290
- Wang HL, Song YP (2008) Behavior of mass concrete under biaxial compression-tension and triaxial compression-compression-tension. *Mater Struct* 42(2):241–249. doi:10.1617/s11527-008-9381-y
- Seow PEC, Swaddiwudhipong S (2005) Failure surface for concrete under multiaxial load: a unified approach. *J Mater Civ Eng ASCE* 17(2):219–228
- Zienkiewicz OC, Owen DRJ, Phillips DV, Nayak GC (1972) Finite element methods in the analysis of reactor vessels. *Nucl Eng Des* 20(2):507–541
- Drucker D, Prager W (1952) Soil mechanics and plastic analysis or limit design. *Q Appl Math* 10(2):157–165
- Pivonka P, Lackner R, Mang HA (2002) Shapes of loading surfaces of concrete models and their influence on the peak load and failure mode in structural analysis. *Int J Eng Sci* 41:1649–1665
- Willam KJ, Warnke EP (1974) Constitutive model for the triaxial behavior of concrete. In: IABSE, Seminar on concrete structures subjected to triaxial stress, Report 19, no. 1 in III. IABSE, Bergamo, Italy, pp 1–30